

# Arabidopsis VILLIN2 and VILLIN3 Are Required for the Generation of Thick Actin Filament Bundles and for Directional Organ Growth<sup>[C][W]</sup>

Hannie S. van der Honing, Henk Kieft, Anne Mie C. Emons, and Tijs Ketelaar\*

Laboratory of Cell Biology, Wageningen University, 6708 PB Wageningen, The Netherlands (H.S.v.d.H., H.K., A.M.C.E., T.K.); and Department of Biomolecular Systems, Stichting voor Fundamenteel Onderzoek der Materie Institute for Atomic and Molecular Physics, 1098 SG Amsterdam, The Netherlands (A.M.C.E.)

In plant cells, actin filament bundles serve as tracks for myosin-dependent organelle movement and play a role in the organization of the cytoplasm. Although virtually all plant cells contain actin filament bundles, the role of the different actin-bundling proteins remains largely unknown. In this study, we investigated the role of the actin-bundling protein villin in *Arabidopsis* (*Arabidopsis thaliana*). We used *Arabidopsis* T-DNA insertion lines to generate a double mutant in which *VILLIN2* (*VLN2*) and *VLN3* transcripts are truncated. Leaves, stems, siliques, and roots of *vln2 vln3* double mutant plants are twisted, which is caused by local differences in cell length. Microscopy analysis of the actin cytoskeleton showed that in these double mutant plants, thin actin filament bundles are more abundant while thick actin filament bundles are virtually absent. In contrast to full-length *VLN3*, truncated *VLN3* lacking the headpiece region does not rescue the phenotype of the *vln2 vln3* double mutant. Our results show that villin is involved in the generation of thick actin filament bundles in several cell types and suggest that these bundles are involved in the regulation of coordinated cell expansion.

The plant actin cytoskeleton plays an essential role in cell division, cytoplasmic organization, cytoplasmic streaming, cell growth, and, consequently, plant morphogenesis. Actin-binding proteins modulate the formation and dynamics of F-actin and its configuration. Among these proteins are the actin-bundling proteins, which are able to cross-link adjacent actin filaments, resulting in bundles consisting of several parallel actin filaments (Thomas et al., 2009). In plant cells, bundling of actin filaments occurs (Thomas et al., 2009), which is likely mediated by actin-bundling proteins. There are four known families of actin-bundling proteins in plants: villins (Vidali et al., 1998; Klahre et al., 2000; Tominaga et al., 2000; Yokota et al., 2003; Huang et al., 2005; Yokota et al., 2005; Khurana et al., 2010; Zhang et al., 2010), fimbrins (Kovar et al., 2000, 2001), formins (Cheung and Wu, 2004; Favery et al., 2004; Michelot et al., 2005; Ye et al., 2009), and LIM proteins (Thomas et al., 2006, 2008; Wang et al., 2008; Papuga et al., 2010). In addition, elongation factor 1 $\alpha$  (Collings et al., 1994; Gungabissoon et al., 2001) has been shown to have actin filament-bundling properties as well. The pres-

ence of these different actin-bundling proteins suggests that their combined actions can result in several types of actin filament bundles, which differ in form and function (Thomas et al., 2009).

Although the roles of the different actin-bundling proteins in the generation of actin filament bundles are not yet known, it is clear that actin filament bundles fulfill several functions in plant cells. Actin filament bundles serve as the preferred tracks for the myosin-dependent movement of organelles (Miller et al., 1999; Ketelaar et al., 2003; Holweg, 2007; Ye et al., 2009). Next to their function in cytoplasmic streaming, actin filament bundles have been shown to play a role in keeping the nucleus at a fixed position from the root hair tip (Ketelaar et al., 2002). Furthermore, actin filament bundles structure the cytoplasm. Their depolymerization causes the collapse of cytoplasmic strands (Staiger et al., 1994; Shimmen et al., 1995; Valster et al., 1997; Hussey et al., 1998; Van Gestel et al., 2002; Higaki et al., 2006; Sheahan et al., 2007; van der Honing et al., 2010), and unbundling results in more, but thinner, cytoplasmic strands (Tominaga et al., 2000; Ketelaar et al., 2002). Thus, actin filament bundles are required to maintain cytoplasmic strand size and number (i.e. the overall organization of the cytoplasm of plant cells).

The genome of *Arabidopsis* (*Arabidopsis thaliana*) contains five villin genes, and the villins encoded by these genes are highly expressed in several tissues of *Arabidopsis* (Klahre et al., 2000). Plant villins are similar to vertebrate villins (Staiger and Hussey, 2004). Villins consist of a core (made up of six tandem

\* Corresponding author; e-mail tijs.ketelaar@wur.nl.

The author responsible for distribution of materials integral to the findings presented in this article in accordance with the policy described in the Instructions for Authors ([www.plantphysiol.org](http://www.plantphysiol.org)) is: Tijs Ketelaar (tijs.ketelaar@wur.nl).

<sup>[C]</sup> Some figures in this article are displayed in color online but in black and white in the print edition.

<sup>[W]</sup> The online version of this article contains Web-only data.

[www.plantphysiol.org/cgi/doi/10.1104/pp.111.192385](http://www.plantphysiol.org/cgi/doi/10.1104/pp.111.192385)

subdomains) and a distinct C-terminal domain, which is referred to as the headpiece. Villin's core shares structural homology to the actin-binding protein gelsolin, which has  $\text{Ca}^{2+}$ -regulated actin filament nucleation, severing, and barbed end capping activity (Bryan and Kurth, 1984; Way et al., 1989). Both the core and the headpiece contain an actin filament-binding domain, and the headpiece region of vertebrate villins has been shown to be essential for actin filament bundling (Glenney and Weber, 1981). This led to the hypothesis that villin bundles actin filaments by acting as a monomer, with the two actin filament-binding domains, one present in the core and the other in the headpiece, cross-linking two adjacent actin filaments (Glenney et al., 1981a). However, one study suggests the presence of a third actin-binding domain, which is present in the core (Hampton et al., 2008), while another study suggests that villin acts as a dimer (George et al., 2007). In addition to their ability to bundle actin filaments, vertebrate villins also show  $\text{Ca}^{2+}$ -dependent actin filament severing, nucleating, and capping (Bretscher and Weber, 1980; Glenney et al., 1981b; Glenney and Weber, 1981) activities. Plant villins also possess actin filament barbed end capping (Yokota et al., 2005; Zhang et al., 2010, 2011), nucleating (Yokota et al., 2005), and severing (Khurana et al., 2010; Zhang et al., 2010, 2011) activities in vitro. Zhang et al. (2011) show that the barbed end capping and severing activities of Arabidopsis VLN4 are  $\text{Ca}^{2+}$  dependent. In plants, villin has been shown to play a role in orga-

nizing the cytoplasm in root hairs (Tominaga et al., 2000; Ketelaar et al., 2002) and pollen tubes (Zhang et al., 2011) as well as in nuclear positioning in root hairs (Ketelaar et al., 2002).

In this study, we analyzed the roles of two Arabidopsis villins using lines with a T-DNA insertion in *VILLIN2* (*VLN2*), *VLN3*, or both *VLN2* and *VLN3*. The *vln2 vln3* double mutants show a clear anomaly in the growth direction of organs, suggesting problems with coordinated cell elongation. The actin cytoskeleton in the double mutants has a finer appearance, and thick bundles of actin filaments are virtually absent. GFP: *VLN3* rescued the morphological phenotype and localizes to actin filament bundles in all cell types studied. We further show that the headpiece region of *VLN3* is important for the localization of *VLN3* to actin filament bundles and for the regulation of directional organ growth. These data show that villin is involved in the generation of thick actin filament bundles and suggest that these bundles are important for the coordination of cell expansion in different organs.

## RESULTS

### T-DNA Insertions in *VLN2* and *VLN3* Result in a Truncated Transcript for Both Genes

A cladogram based on cDNA sequences shows that *VLN2* (At2g41740) and *VLN3* (At3g57410) belong to the same clade (Fig. 1A), suggesting that they have

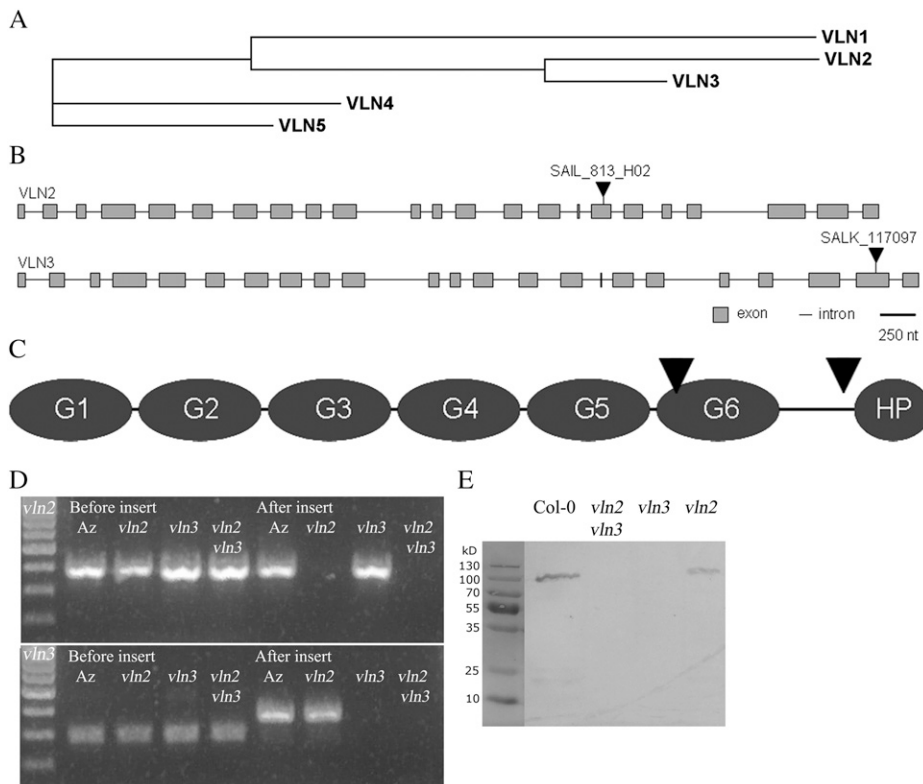


**Figure 1.** Characterization of the Arabidopsis villin gene family and T-DNA insertions in *vln2* and *vln3*. A, Cladogram of the Arabidopsis villins, based on cDNA sequences. B, Locations of T-DNA inserts in *vln2* and *vln3*. Gray boxes represent exons, and horizontal lines represent introns. T-DNA inserts (arrowheads) are not drawn to scale. C, Domain structure of villin. Arrowheads show locations corresponding to the locations of T-DNA inserts of *vln2* and *vln3*. D, T-DNA insertions result in truncated transcripts in *vln2*, *vln3*, and *vln2 vln3*. Products could be amplified using a cDNA template using *VLN*-specific primers before the inserts, but when both primers (*vln2*) or the reverse primer (*vln3*) were designated for coding regions after the insert (Supplemental Fig. S3; Supplemental Table S1), products could not be amplified. Az, Azygous. E, A protein gel blot of Col-0, *vln2*, *vln3*, and *vln2 vln3* root extracts probed with lily anti-villin antibody (Tominaga et al., 2000) shows that *vln3* and *vln2 vln3* do not contain (a truncated version of) the *VLN3* protein.

arisen from a relatively recent genome duplication. They share 84% similarity in their cDNA sequences and 80% similarity in their amino acid sequences. Both *VLN2* and *VLN3* are expressed in all organs ([www.bar.utoronto.ca](http://www.bar.utoronto.ca)), with similar expression levels for both villins in most organs. *VLN2* has a slightly higher expression level in mature pollen grains.

To test the biological roles of *VLN2* and *VLN3*, lines homozygous for T-DNA insertions in *VLN2* and *VLN3* were identified. The T-DNA insertions for both *vln2* and *vln3* (i.e. SAIL\_813\_H02 and SALK\_117097, respectively) are located in exons (Fig. 1B), at locations corresponding to the G6 domain in *vln2* and to the linker domain between the G6 and headpiece domains in *vln3* (Fig. 1C), according to Klahre et al. (2000). The presence of *VLN2* and *VLN3* transcripts was tested using reverse transcription-PCR in both azygous (homozygous for the undisrupted gene) and mutant plants from the same population. Primer combinations before and after the inserts were used to test if transcripts were present, truncated, or absent. For both *vln2* and *vln3*, transcripts corresponding to coding regions before the insert were present, but the region after the insert was not transcribed (Fig. 1D). Thus, the presence of the inserts results in truncated transcripts for both *VLN2* and *VLN3*. We generated a double mutant of these lines with truncated mRNA for both genes (Fig. 1D).

Although the presence of the T-DNA inserts results in truncated transcripts for both *VLN2* and *VLN3*, the corresponding proteins could be absent. We tested this by probing a protein gel blot of wild-type Columbia-0 (Col-0), *vln2*, *vln3*, and *vln2 vln3* root extracts with a polyclonal anti-lily (*Lilium longiflorum*) villin antibody (Tominaga et al., 2000; Ketelaar et al., 2002; Khurana et al., 2010). This resulted in a band at a height corresponding to the predicted mass of *VLN3* (107 kD) in Col-0 and *vln2* extracts, but in *vln3* and *vln2 vln3* extracts, no band was visible (Fig. 1E). The absence of a band at a height corresponding to a smaller protein shows that *vln3* and *vln2 vln3* do not contain detectable amounts of the truncated version of *VLN3*. Thus, although these lines contain a truncated *VLN3* transcript (Fig. 1D), the *VLN3* protein is absent or a truncated protein is produced at levels below the western-blotting detection limit. The absence of a villin band in the root extract of the *vln3* plant shows that the antibody does not recognize the *VLN2* protein. We conclude that while *vln2* and *vln2 vln3* might contain a truncated version of *VLN2*, *vln3* and *vln2 vln3* do not contain detectable amounts of the full-length or truncated *VLN3* protein.

#### Arabidopsis Plants Homozygous for a T-DNA Insertion in Two Villin Genes Display Defects in Directional Organ Growth

Seedlings of single mutants of *vln2* and *vln3* do not show any developmental defects or delays, but those of *vln2 vln3* double mutants have curly roots (Fig. 2A).

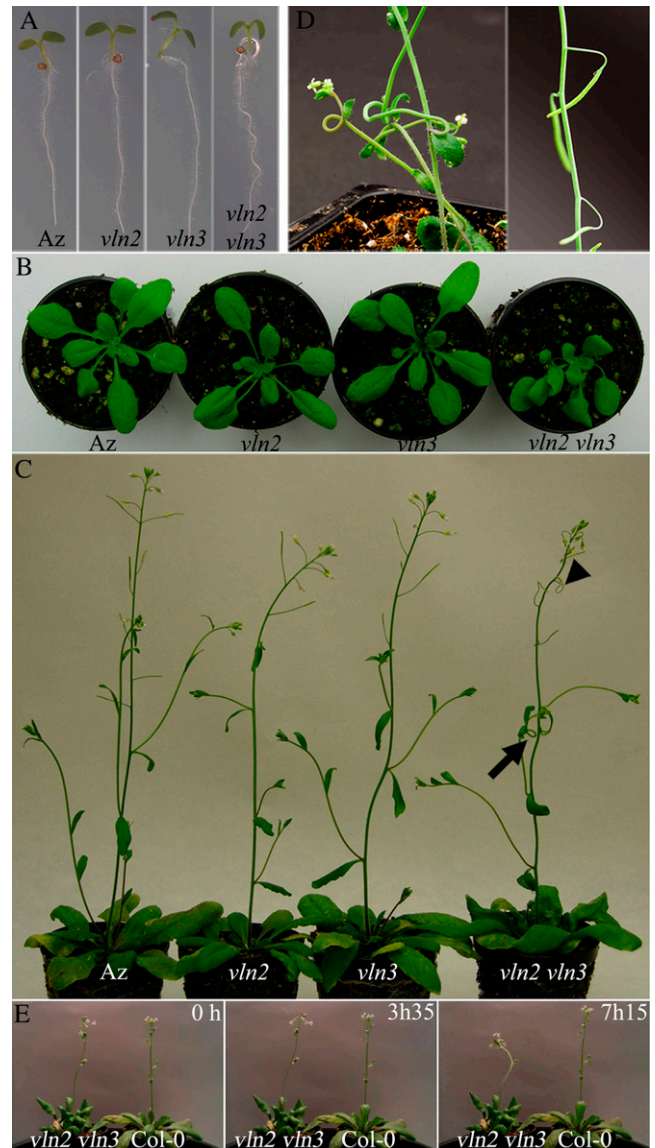


**Figure 2.** Phenotype of *vln2 vln3*. A, Root morphology of azygous, (Az), *vln2*, *vln3*, and *vln2 vln3* plants. Roots of both single mutants have the same appearance as azygous roots, but roots of double mutants grow in a curly, wavy manner. B, Phenotypes of 2-week-old plants. Leaves of the *vln2 vln3* double mutant are twisted, but in single mutants, this twisting is absent. C, Phenotypes of 5-week-old plants. Branches of single mutants grow straight, similar to those of azygous plants, but in the double mutants, branches are curly and even show complete twists (arrow). This twisting also occurs in the fruit stalks. D, Twisting of double mutant branches and fruit stalks shown at a higher magnification. E, The rotational movements (circumnutation) of *vln2 vln3* inflorescences have larger amplitudes than those of Col-0 inflorescences and are less regular (Supplemental Movie S1). [See online article for color version of this figure.]

Plant growth and organ development in the double mutant occur at similar rates as those of azygous plants and single mutants, and the production of viable seeds is unaffected by the presence of T-DNA insertions in both genes. However, rosette leaves of the

double mutant are twisted (Fig. 2B). In addition, stems of the *vln2 vln3* double mutant are curly, and inflorescences show complete turns (Fig. 2, C and D). Both single mutants do not show this phenotype. The tops of the growing inflorescences of the double mutant are often (41%;  $n = 17$ ) oriented downward, while this never occurs in Col-0 plants ( $n = 22$ ) or single mutants ( $n = 19$  for *vln2* and 17 for *vln3*; Fig. 3A). Time-lapse recording of Col-0 and *vln2 vln3* plants shows that the rotational movements (circumnutation) of *vln2 vln3* inflorescences differ from those of Col-0 inflorescences: in the double mutant, periods of normal circumnutation alternate with periods in which the circumnutation movements show larger amplitudes than those of Col-0 (Fig. 2E; Supplemental Movie S1). Although hypocotyls from light-grown seedlings do not show any defects, etiolated hypocotyls appear curly, similar to other organs (Supplemental Fig. S1, A and B). These data suggest that the coordination of cell expansion in the organs is affected in *vln2 vln3*, resulting in the curly phenotype of roots, leaves, etiolated hypocotyls, and inflorescences. Siliques and fruit stalks of *vln2 vln3* were also curly (Fig. 2, C and D), and 59% of the siliques were oriented at angles smaller than  $90^\circ$  with respect to the plant axis ( $n = 80$ ), while this rarely occurred (with a maximum of 6%) in Col-0 plants ( $n = 49$ ) or single mutants ( $n = 50$ ; Fig. 3B). Despite the curly phenotype of leaves and fruit stalks, only the width of fruit stalk

epidermal cells is slightly, but significantly, higher in the double mutant ( $0.99 \pm 0.25 \mu\text{m}$  in *vln2 vln3* compared with  $0.88 \pm 0.23 \mu\text{m}$  in Col-0; Student's  $t$  test,  $P = 0.01$ ). The surface area, perimeter, and circularity (Brembu et al., 2004) of abaxial leaf pavement cells ( $n = 26$  for Col-0 and 61 for *vln2 vln3*; Fig. 3C) and the surface area, perimeter, length, and circularity of fruit stalk epidermal cells ( $n = 68$  for Col-0 and 67 for *vln2 vln3*; Fig. 3D) are not affected by the mutations in *VLN2* and *VLN3*. The gravitropic response in the *vln2 vln3* double mutant is not affected (Supplemental Fig. S1, C and D). In addition, trichome size, shape, and branch numbers are normal in the *vln2 vln3* double mutant.

To determine the cause of the organ-curling phenotype, we stained roots with  $1 \mu\text{g mL}^{-1}$  propidium iodide and measured cell lengths of fully grown root epidermal cells of different cell files of the inner and outer sides of a curve in the root. In wild-type roots, we did not observe these curves and did not find differences in cell lengths between cells of the different cell files ( $193 \pm 30 \mu\text{m cell}^{-1}$ ). The lengths of *vln2 vln3* root epidermal cells are significantly different in cell files of the inner and outer sides of a root curve (cell lengths were  $195 \pm 35 \mu\text{m}$  in outer cell files and  $182 \pm 40 \mu\text{m}$  in inner cell files). Lengths of 20 root epidermal cells on the inner or outer side of a root curve were measured in 13 (outer side) and 10 (inner side) roots. The average cell lengths of the different roots were

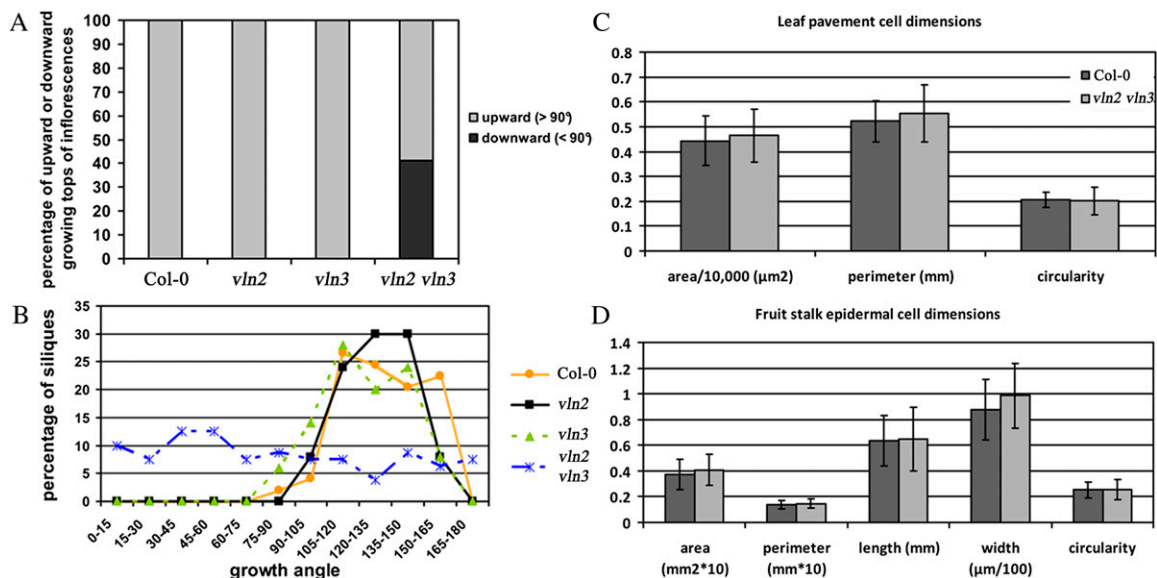


**Figure 3.** Quantification of the *vln2 vln3* phenotype. A, A total of 41% ( $n = 17$ ) of the tops of inflorescence meristems of *vln2 vln3* grow downward, while this never occurs in Col-0 ( $n = 22$ ) and single mutant ( $n = 19$  for *vln2* and 17 for *vln3*) plants. B, The angle of siliques with respect to the plant axis of the *vln2 vln3* double mutant is less regular than that of Col-0 and single mutant plants: siliques of *vln2 vln3* grow in all directions at similar frequencies, while those of Col-0 and single mutant plants preferentially grow upward at an oblique angle. C and D, Leaf pavement (C;  $n = 26$  for Col-0 and 61 for *vln2 vln3*) and fruit stalk epidermal (D;  $n = 68$  for azygous and 67 for *vln2 vln3*) cell dimensions of *vln2 vln3* are similar (Student's  $t$  test,  $P > 0.05$ ) to those of Col-0 plants, except for fruit stalk epidermal cell width, which is significantly higher (Student's  $t$  test,  $P = 0.01$ ) to that in *vln2 vln3*. Circularity reflects the ratio of cell area to cell perimeter and is defined as  $4\pi \text{ area/perimeter}^2$  (Vidali et al., 2007). Error bars in C and D represent sd. [See online article for color version of this figure.]



used to determine the significance of the difference. An unpaired *t* test shows that the difference is highly significant ( $P < 0.001$ ). Thus, the organ curling occurs through local differences in cell expansion.

Although *VLN2* and *VLN3* are both expressed in root hairs ([www.bar.utoronto.ca](http://www.bar.utoronto.ca)), we did not observe differences from Col-0 plants in root hair morphology (Supplemental Fig. S2A), nucleus-to-tip distance (Supplemental Fig. S2B), and growth rate (Supplemental Fig. S2C) of elongating root hairs of the double mutant. Thus, the mutations in *VLN2* and *VLN3* do not affect the growth and morphology of individual cells, such as root hairs and trichomes, but do result in defects in the directional growth of roots, shoots, leaves, and siliques. This suggests that the mutations affect coordinated cell elongation.

To confirm that the observed morphological phenotype is caused by the presence of the T-DNA inserts in *VLN2* and *VLN3*, we complemented the mutant phenotype with genomic *VLN2* and *VLN3*, under the control of their endogenous promoters, and with *PVLN3:VLN3* cDNA. In most transformants carrying these constructs, the mutant phenotype was fully rescued (genomic *VLN2*, 27 out of 34 independent transformants; genomic *VLN3*, 26 out of 29 independent transformants; *PVLN3:VLN3* cDNA, 38 out of 45 independent transformants; Supplemental Fig. S3). These results confirm that the defects in directional organ growth are caused by the combined mutations in *VLN2* and *VLN3*. Thus, *VLN2* and *VLN3* play a redundant role in the regulation of directional organ growth.

#### Thick Actin Filament Bundles Are Virtually Absent in *vln2 vln3*, while Thin Bundles Are More Abundant

To investigate if the actin organization is affected by the presence of the T-DNA insertions in *VLN2* and *VLN3*, we used *GFP:FABD2* (Ketelaar et al., 2004) expression to visualize actin filaments in cells of the single mutants and the double mutant and compared the actin organization with that of Col-0 cells. We experienced silencing problems when we tried to cross *GFP:FABD2* expression into the *vln2 vln3* double mutant (the F2 from *vln2* and *vln3* single mutants segregated as expected: approximately 25% of the plants were homozygous for *vln2* or *vln3* and one in four of the homozygous plants expressed *GFP:FABD2*). In the F2 of the cross of *GFP:FABD2* and the *vln2 vln3* double mutant, we found that approximately one in 16 plants showed the mutant phenotype as expected (115 out of 1,889 F2 plants), but none of these plants showed *GFP:FABD2* expression, whereas *GFP:FABD2* expression is expected in 75% of the F2 lines homozygous for *vln2 vln3*. Over 90% of the F1 plants of this cross showed *GFP:FABD2* expression. Hence, we resorted to transforming the *35S::GFP:FABD2* construct directly into the *vln2 vln3* double mutant. This approach resulted in 202 independent transformants. Most (198) transformants did not show any *GFP:FABD2* expression. Only

four of these lines occasionally showed *GFP:FABD2* expression in several cells. We used these lines to study actin organization in the *vln2 vln3* double mutant. The actin organization in fully elongated hypocotyl epidermal cells of the single mutants is similar to that of wild-type cells: thick, predominantly longitudinal actin filament bundles are interspersed with a more complex network of thinner bundles (Fig. 4, A–I). In the double mutant, however, the thick, longitudinal actin filament bundles are absent and thinner bundles are more abundant. Fully elongated root and abaxial leaf epidermal cells of the double mutant also appear to contain more thin bundles of actin filaments than those in azygous plants and the single mutants, while thick actin filament bundles are absent (Fig. 4, J–L).

To quantify the observed differences in actin organization, we created intensity profiles of GFP fluorescence of *P35S::GFP:FABD*-expressing hypocotyl cells ( $n = 8$  for Col-0 and *vln2 vln3*), in the middle of Z projections of the cortical cytoplasm, perpendicular to the longitudinal cell axis (excluding the bright cell edges; Fig. 4, M–O). In these intensity profiles, high peaks represent brightly labeled actin filament bundles, while low peaks represent weakly labeled actin filament bundles (or perhaps single actin filaments, although it is unlikely that single actin filaments are detectable with the setup used). We counted the number of peaks per micrometer and distributed these peaks in three classes: high, medium, and low gray levels (Fig. 4P).

The frequency distribution of the number of peaks across the three classes was clearly different between Col-0 and *vln2 vln3* hypocotyl cells. A total of 17% of the peaks in Col-0 cells belonged to the class with the highest intensity levels, representing thick actin filament bundles, while in *vln2 vln3*, only 2% of the peaks represented this class (Fig. 4O). Peaks with a low fluorescence intensity were more abundant in *vln2 vln3* (70%) than in Col-0 (47%) cells. A Pearson's  $\chi^2$  test showed that the frequency distribution across the three classes was significantly different between Col-0 and *vln2 vln3* cells ( $P < 0.001$ ). The average number of peaks per micrometer was higher (*t* test;  $P = 0.04$ ) in the double mutant ( $0.82 \pm 0.29$ ) than in Col-0 cells ( $0.51 \pm 0.26$ ; Fig. 4Q). Besides this analysis, we used the analysis method designed by Higaki et al. (2010) to assess differences in the degree of actin filament bundling. We determined skewness, which is a parameter that represents the amount of bundling (higher values indicate the presence of thicker bundles), and occupancy, which gives insight into the density of the actin cytoskeleton. Analysis was performed as described in "Materials and Methods" and resulted in a skewness of  $1.86 \pm 0.29$  in hypocotyl epidermal cells of Col-0 plants ( $n = 100$  cells from seven different plants) and  $0.73 \pm 0.31$  in these cells of the *vln2 vln3* mutant ( $n = 50$  cells from 30 different plants). This difference is highly significant (unpaired *t* test;  $P < 0.0001$ ). The occupancy in hypocotyl epidermal cells of Col-0 plants was  $0.23 \pm$

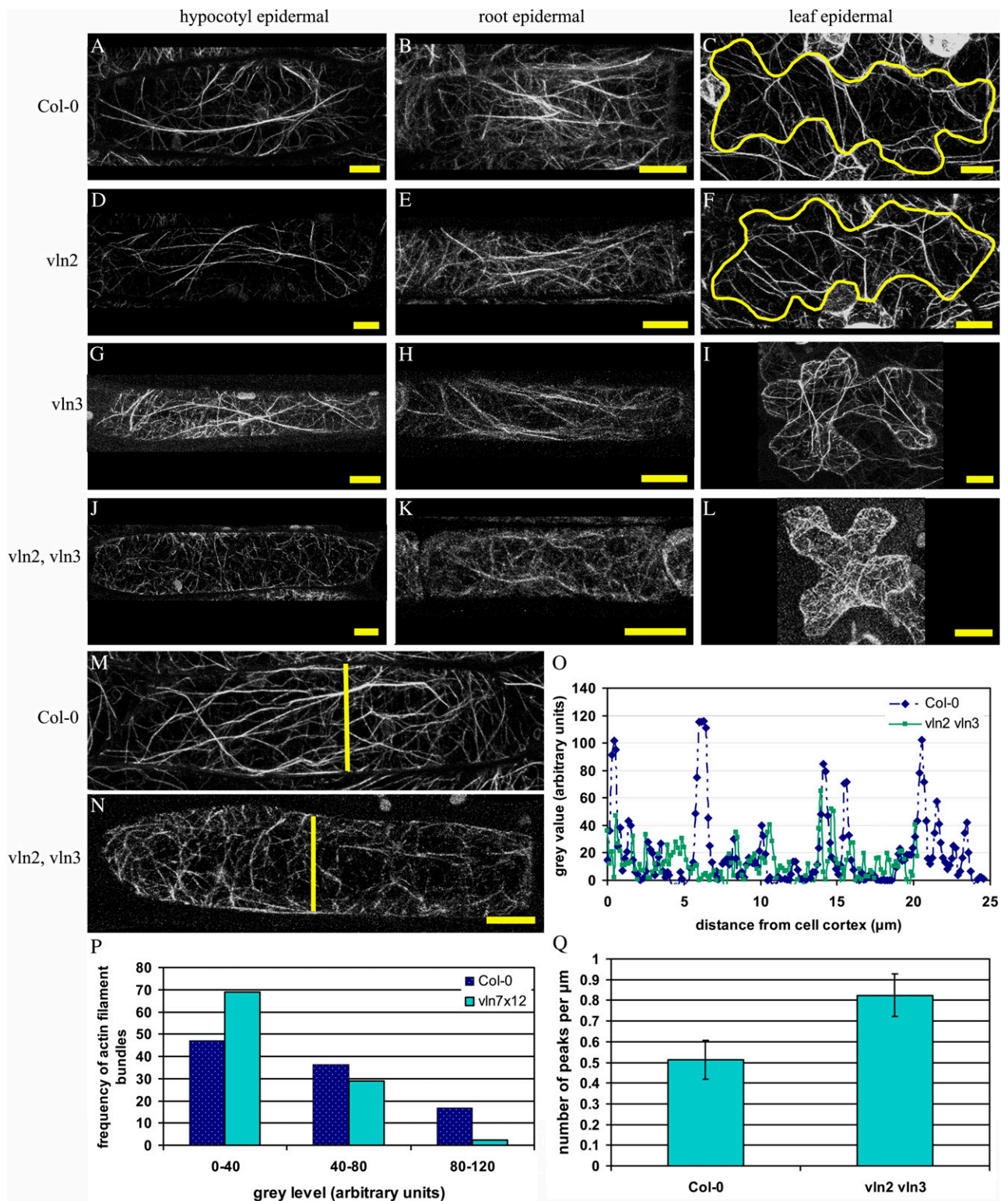


**Figure 4.** Thick actin bundles are absent in *vln2 vln3*, but thin bundles of actin filaments are more prominent. A to L, The actin organization (visualized with GFP:FABD2) in cells of both single mutants (D–I) is similar to that in Col-0 cells (A–C): thick bundles of actin filaments alternate with a more complex network of thin (bundles of) actin filaments. In the double mutant (J–L), thick actin filament bundles appear to be absent, while thin actin filament bundles seem more prominent. M to O, Representative intensity profiles of fluorescence intensity in a Col-0 (M) and a *vln2 vln3* (N) fully elongated hypocotyl cell. High peaks represent thick actin filament bundles, while lower peaks represent thinner bundles. The yellow lines in M and N show the locations of the

0.024 compared with  $0.41 \pm 0.079$  in those of the *vln2 vln3* mutant. Also, this difference is highly significant (unpaired *t* test;  $P < 0.0001$ ). The skewness and occupancy of the actin cytoskeleton in *vln2* and *vln3* single mutants did not differ significantly from that in Col-0 plants (*vln2*, skewness of  $1.95 \pm 0.35$  [unpaired *t* test;  $P = 0.12$ ] and occupancy of  $0.21 \pm 0.130$  [unpaired *t* test;  $P = 0.14$ ;  $n = 50$  cells from seven plants]; *vln3*, skewness of  $1.80 \pm 0.45$  [unpaired *t* test;  $P = 0.33$ ] and occupancy of  $0.23 \pm 0.031$  [unpaired *t* test;  $P = 1.0$ ;  $n = 50$  cells from five plants]). We conclude that cells of the double mutant, but not the single mutants, contain more thin bundles of actin filaments than Col-0 cells, while the average thickness of these bundles is thinner.

To test whether the defects in actin organization occur during cell expansion and correlate with the defects in organ growth, we studied the actin organization in elongating root epidermal cells in Col-0 and *vln2 vln3* plants (Fig. 5). Similar to the actin organization in fully grown cells, the skewness and occupancy of the actin cytoskeleton in these cells were significantly different (Col-0, skewness of  $1.34 \pm 0.38$  and occupancy of  $0.15 \pm 0.009$ ; *vln2 vln3*, skewness of  $0.43 \pm 0.19$  and occupancy of  $0.57 \pm 0.11$  [unpaired *t* test;  $P < 0.0001$  for both skewness and occupancy]; Col-0,  $n = 50$  cells from seven different plants; *vln2 vln3*,  $n = 35$  cells from 20 different plants).

#### GFP:VLN3 Labels Some (Bundles of) Actin Filaments

To determine the subcellular localization of villin, we complemented the double mutant with *GFP:VLN3*, expressed under the control of the endogenous promoter (*PVLN3:GFP:VLN3* genomic). Expression of this construct in the mutant rescued the phenotype in 88 out of 99 independent transformants, showing that the fusion protein is functional. *GFP:VLN3* is present in all investigated cells: leaf, hypocotyl, and root epidermal cells, including root hairs (Fig. 6). In all these cell types, *GFP:VLN3* partly shows a cytoplasmic localization. Besides this cytoplasmic localization, *GFP:VLN3* localizes to filamentous structures resembling (bundles of) actin filaments both in the cortical cytoplasm and in cytoplasmic strands of the cells studied (Fig. 6, A–D). Coexpression of *PVLN3:GFP:VLN3* and *P35S:mCherry:FABD2* in tobacco (*Nicotiana benthamiana*) leaves demonstrates that *GFP:VLN3* and *mCherry:FABD2* colocalize (Fig. 6, E–G), confirming that *GFP:VLN3* localizes to actin filaments. Villin appears not to label all actin filament bundles equally strongly (Fig. 6, E–G). In growing root hairs, *GFP:VLN3* localizes to the long

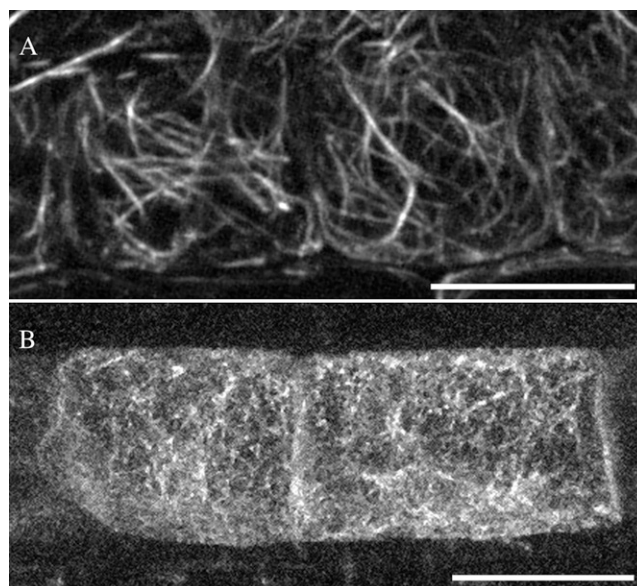


**Figure 5.** The irregular organ growth phenotype correlates with defects in actin organization in expanding cells. The actin organization in elongating root epidermal cells of the *vln2 vln3* mutant (B) is disrupted when compared with the actin organization of Col-0 cells (A). The defects in actin organization resemble those in fully grown cells. The actin organization is visualized by *GFP-FABD2* expression. Bars = 20  $\mu\text{m}$ .

actin filament bundles oriented longitudinally to the cell's long axis in the root hair tube (Fig. 6D). These actin filament bundles do not penetrate the (sub)apical region. Image sequences of root epidermal cells collected at 5-s intervals (Fig. 6, H–J; Supplemental Movie S2) or of root hairs at 30-s intervals (Fig. 6, K–M; Supplemental Movie S3) show that the actin filament bundles to which *VLN3* localizes relocate over time.

#### The Headpiece Region of *VLN3* Is Required for the Bundling of Actin Filaments

Next to its actin filament-bundling capacity, which is independent of  $\text{Ca}^{2+}$  levels (Khurana et al., 2010), *VLN3* has actin filament severing properties, and this activity is  $\text{Ca}^{2+}$  dependent (Khurana et al., 2010). Since the mutations in *VLN2* and *VLN3* result in an actin cytoskeleton organization that is virtually devoid of thick actin filament bundles, we propose that the absence of villin's bundling activity plays a major role in causing the morphological phenotype. The fact that

#### Figure 4. (Continued.)

intensity profile in O. P. Frequency distribution of peaks belonging to three fluorescence intensity classes (determined for six cells for each genotype) in Col-0 and *vln2 vln3*. In Col-0 cells, peaks with a fluorescence intensity of 80 to 120 (representing thick actin filament bundles) are more abundant than in *vln2 vln3*, while peaks with a fluorescence intensity of 0 to 40 (representing thin[er] actin filament bundles) are more abundant in *vln2 vln3*. Q, The number of peaks per micrometer shown for Col-0 and *vln2 vln3*. *vln2 vln3* cells contain significantly more (Student's *t* test,  $P = 0.04$ ) actin filament bundles than Col-0 cells. Bars in A to N = 10  $\mu\text{m}$ . Error bars in Q represent *se*. [See online article for color version of this figure.]



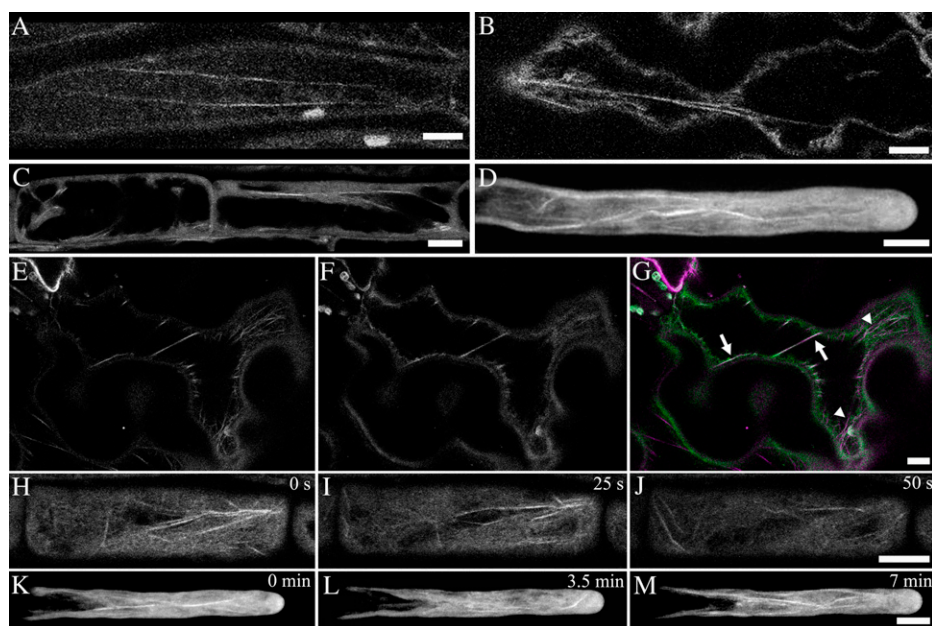


**Figure 6.** GFP:VLN3, expressed under the control of the *VLN3* promoter, localizes to (bundles of) actin filaments. A to D, Representative images of complemented *vln2 vln3* plants show that besides a cytoplasmic localization, GFP:VLN3 decorates (bundles of) actin filaments in hypocotyl epidermal (A), leaf epidermal (B), and root epidermal (C and D) cells. These images show fully grown hypocotyl epidermal (A) and leaf epidermal (B) cells and elongating root epidermal cells (C and D). In growing root hairs (D), GFP:VLN3 localizes to the long actin filament bundles oriented longitudinally to the cell's long axis in the root hair tube. E to G, Coexpression of *PVLN3:GFP:VLN3* and *P35S:mCherry:FABD2* in tobacco demonstrates that GFP:VLN3 (E) and mCherry:FABD2 (F) colocalize (arrows) in leaf epidermal cells, although GFP:VLN3 does not localize to all actin filaments (arrowheads). G shows an overlay of E and F (GFP:VLN3, green; mCherry:FABD2, magenta). Image sequences of elongating root epidermal cells (H–J) and root hairs (K–M) of complemented *vln2 vln3* plants show that GFP:VLN3 localizes to (bundles of) actin filaments that reorganize over time. See also Supplemental Movies S2 and S3. Bars = 10  $\mu\text{m}$ . [See online article for color version of this figure.]

the mutations affect the actin cytoskeleton organization also at locations where  $\text{Ca}^{2+}$  is at the basal level, while VLN3 shows only severing activity at high  $\text{Ca}^{2+}$  concentrations (Khurana et al., 2010), is in agreement with the hypothesis that villin's bundling activity rather than its severing activity causes the developmental problem in the double mutant. It is likely that plant villins require the headpiece region for actin filament bundling. Both the core and the headpiece region of vertebrate villins can bind to F-actin, and the headpiece region of vertebrate villin is crucial for its bundling capacity (Glennay and Weber, 1981). Therefore, we hypothesized that in plant cells, villin's headpiece region plays an important role in the generation of actin filament bundles. To obtain more insight into the function of the headpiece region of Arabidopsis VLN3, we performed a complementation analysis with three different constructs lacking the DNA that encodes the villin headpiece region, all driven by the endogenous *VLN3* promoter: *PVLN3:VLN3 $\Delta$ HP* genomic, *PVLN3:GFP:VLN3 $\Delta$ HP* genomic, and *PVLN3:GFP:VLN3 $\Delta$ HP* cDNA. All these constructs were unable to rescue the phenotype (*PVLN3:VLN3 $\Delta$ HP* genomic, 43 independent transformants; *PVLN3:GFP:VLN3 $\Delta$ HP* genomic, 56 independent transformants; *PVLN3:GFP:VLN3 $\Delta$ HP* cDNA, 34 independent trans-

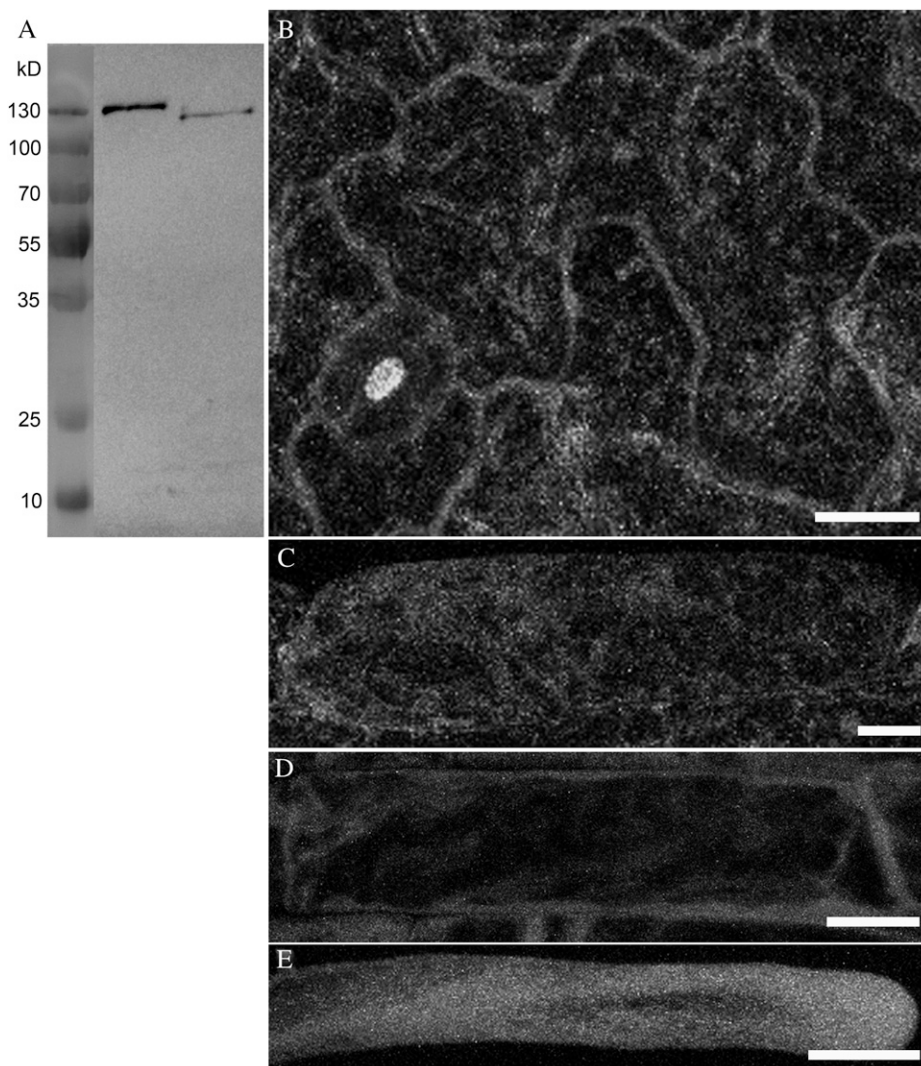
formants). In addition, in contrast to GFP:VLN3, which localizes to (bundles of) actin filaments, GFP:VLN3 $\Delta$ HP fluorescence is equally distributed throughout the cytoplasm (Fig. 7). To test whether the cytoplasmic fluorescence represents full-length GFP:VLN3 $\Delta$ HP, we performed western blotting with an antibody against GFP. Figure 7A shows that plants expressing VLN3 $\Delta$ HP produce a fusion protein of approximately 120 kD, which is the expected mass of GFP:VLN3 $\Delta$ HP. This shows that the cytoplasmic distribution is due to the absence of the headpiece and is not caused by truncations in the GFP:VLN3 $\Delta$ HP gene product. We conclude that VLN3 requires the headpiece region for a correct localization to actin filament bundles, for actin filament bundling, and for its function in directional organ growth.

## DISCUSSION

The actin cytoskeleton plays a key role in plant cell growth and morphogenesis. Although in virtually all plant cells, actin filament bundling occurs (Thomas et al., 2009), it is unknown how actin filament bundles are generated by actin-bundling proteins. In this study, we investigated the role of two villins in Arabidopsis



**Figure 7.** GFP:VLN3 $\Delta$ HHP, expressed under the control of the *VLN3* promoter, shows a cytoplasmic localization. A, Western blotting with an anti-GFP antibody reveals that GFP:VLN3-expressing plants express a fusion protein of approximately 137 kD, the expected mass of GFP:VLN3. GFP:VLN3 $\Delta$ HHP-expressing plants express a fusion protein of approximately 120 kD, which is the expected mass of GFP:VLN3 $\Delta$ HHP. B to E, Representative images of leaf epidermal (B), hypocotyl epidermal (C), and root epidermal (D) cells and a root hair (E) of *vln2 vln3* plants in which *GFP:VLN3 $\Delta$ HHP* is expressed. In these plants, which are not rescued, GFP:VLN3 $\Delta$ HHP fluorescence is equally distributed throughout the cytoplasm. Bars = 10  $\mu$ m.



and show that the absence of these villins results in a low abundance of thick actin filament bundles. *vln2 vln3* plants have twisted leaves, stems, siliques, and roots, implying an important role for villin in the regulation of directional organ growth. Truncated VLN3 lacking the headpiece region, in contrast to full-length VLN3, is not able to rescue the phenotype, and in vitro experiments show that the headpiece region is essential for actin filament bundling. These data show that villin is involved in the generation of actin filament bundles and suggest that villin-mediated actin filament bundling is required for the regulation of coordinated cell expansion.

#### VLN2 and VLN3 Play a Role in Actin Filament Organization in Arabidopsis

The presence of the T-DNA insertions in *VLN2* and *VLN3* affects the actin organization in several cell types. In cells of the double mutant, thick actin filament bundles are virtually absent, whereas thin bun-

dles are more abundant. The fact that the double mutant still contains thin actin filament bundles points to the combined action of VLN2 and VLN3 with that of another actin-bundling protein in the generation of actin filament bundles in plant cells. Since *VLN5* is preferentially expressed in pollen (Zhang et al., 2010), *VLN1* and *VLN4* are good candidates to work cooperatively with VLN2 and VLN3. Alternatively, another class of actin-bundling proteins could be involved in the generation of actin filament bundles in plant cells. In vertebrate cells, different actin-bundling proteins also are generally present in the same actin filament bundles (Tilney et al., 1998; Bartles, 2000), and these proteins do not act redundantly. In vitro experiments showed that small rigid actin-bundling proteins can generate small bundles with a finite thickness of approximately 20 filaments (Claessens et al., 2008). Other actin-bundling proteins were shown to be able to link these small bundles into larger bundles of several hundreds of actin filaments (Claessens et al., 2008). In plants, actin filament bundles could be gen-

erated in a comparable way. Villins might work coordinately with fimbrins (Kovar et al., 2000), formins (Cheung and Wu, 2004; Favery et al., 2004; Michelot et al., 2005; Ye et al., 2009), LIM proteins (Thomas et al., 2006, 2007), and/or elongation factor 1 $\alpha$  (Collings et al., 1994) in the formation of thick actin filament bundles. Consistent with this idea, fimbrin has been proposed to cross-link actin filament bundles generated by other actin-bundling proteins, such as villin (Matova et al., 1999; Wu et al., 2010). The silencing of *GFP:FABD2* expression in the *vln2 vln3* double mutant that we observed could be a consequence of the simultaneous inhibition of *VLN2* and *VLN3* expression and the disruption of fimbrin binding to actin filaments by *GFP:FABD2*, which consists of the second actin-binding domain of Arabidopsis fimbrin 1 (Ketelaar et al., 2004). Together, these disruptions may cause insurmountable actin-bundling problems.

Interestingly, the *vln2 vln3* double mutant does not display a trichome phenotype. Trichome development is strongly affected by disruption of the actin cytoskeleton, resulting in distorted trichomes (Mathur et al., 1999; Szymanski et al., 1999). The Arp2/3 complex has been identified as a key factor in actin organization in trichomes and trichome development (Le et al., 2003; Li et al., 2003; Mathur et al., 2003). Since actin defects cause a well-defined trichome phenotype that is absent in the *vln2 vln3* double mutant, together with the lack of detectable *PVLN3:GFP:VLN3* expression in trichomes, it is unlikely that *VLN2* and *VLN3* contribute to actin organization during trichome development.

Besides of villin's role in actin filament bundling, it is likely to play additional roles in actin organization. In addition to its bundling capacity, which is independent on  $Ca^{2+}$  levels, *VLN3* has been shown to have actin filament severing properties, and this activity is  $Ca^{2+}$  dependent (Khurana et al., 2010). *VLN4*, which is expressed in root hairs (Zhang et al., 2011), and *VLN5*, which is highly expressed in pollen tubes (Zhang et al., 2010), have similar properties: they both bundle actin filaments in a  $Ca^{2+}$ -independent manner but have actin filament severing capacity only at high (micromolar and millimolar)  $Ca^{2+}$  concentrations (Zhang et al., 2010). In addition, these villins have actin filament capping activity. The lily villin P-135-ABP has been shown to have actin filament nucleating, depolymerizing, and capping activities, and these activities were  $Ca^{2+}$ /calmodulin dependent. Although the authors state that the nucleating capacity is probably not relevant in vivo (since the nucleation was not accelerated when G-actin was saturated with profilin, which is the case in plant cells), the depolymerizing and capping activities might enhance actin dynamics in the apical region of tip-growing cells, where  $Ca^{2+}$  is abundant (Yokota et al., 2005). Zhang et al. (2011) predicted that *VLN4*, which is involved in the generation and/or maintenance of actin filament bundles in the shank of root hairs (Zhang et al., 2011), participates in the regulation of actin cytoskeleton organization in the subapical and apical regions of root hairs by its

bundling, capping, and/or severing activities. Likewise, *VLN5* has been proposed to bundle actin filaments in the shank of pollen tubes, while enhancing actin dynamics in the apical region, by severing and capping of actin filaments (Zhang et al., 2010). *VLN3* (and perhaps also *VLN2*) could, besides being involved in the generation of actin filament bundles, locally also play a role in enhancing actin dynamics.

Although the localization of *GFP:VLN3* to (bundles of) actin filaments in the shank of root hairs shows that *VLN3* is expressed in root hairs, root hair growth and morphology, which are very sensitive to changes in actin filament organization, are not affected by the mutations in *VLN2* and *VLN3*. This might mean that the proteins act redundantly with another villin in root hairs. *VLN5* is preferentially expressed in pollen and pollen tubes (Zhang et al., 2010) and therefore is not likely to act redundantly with *VLN2* and *VLN3* in root hairs. *VLN1*, which is  $Ca^{2+}$  independent, has only actin filament-bundling capacity (Huang et al., 2005), and *VLN3* can sever actin filament bundles in the presence of *VLN1* (Khurana et al., 2010), showing that the activities of *VLN1* and *VLN3* are not completely redundant. If *VLN2* and *VLN3* act redundantly with another villin in root hairs, *VLN4*, which is involved in actin filament bundling in root hairs (Zhang et al., 2011), would therefore be the best candidate. Alternatively, the fact that root hair growth and morphology are not affected by the mutations in *VLN2* and *VLN3* could mean that these villins are not essential for root hair growth and morphology. In intercalary growing cells, *VLN2* and *VLN3* are essential for the organization of actin filaments. Thick actin filament bundles are virtually absent in cells of the *vln2 vln3* double mutant, and our data show that villin requires the headpiece region for localizing to (bundles of) actin filaments in vivo. This implies that although villin may play additional roles in actin organization, for instance by actin filament severing, villin's bundling capacity plays a major role in its function in actin filament organization.

#### Actin Filament Organization Is Required for Plant Growth Polarity

The actin cytoskeleton plays a key role in plant cell growth. It plays a fundamental role in the delivery of growth materials to exocytosis sites (Miller et al., 1997; Geitmann and Emons, 2000; Vidali and Hepler, 2001) not only because (bundles of) actin filaments serve as tracks for cytoplasmic streaming but also because they optimize the cytoplasmic organization for cell growth. In addition, fine F-actin is thought to be important for the filtering and delivery of Golgi-derived vesicles (Miller et al., 1999) that contain cell wall matrix materials in their lumen and the enzymes for callose and cellulose production in their membrane. Our data show that the activities of *VLN2* and *VLN3* are required for the organization of the actin cytoskeleton. In the absence of *VLN2* and *VLN3* proteins, thick actin filament bundles are virtually absent, while fine bun-

dles are more abundant. Cell shapes and sizes and plant growth rates are similar in Col-0 and double mutant plants. This shows that the thick actin filament bundles that are absent in the double mutant are not essential for cell and plant growth. However, the wavy, twisted appearance of several organs in the double mutant, and the larger amplitudes of the rotational movements (circumnutation) of double mutant inflorescences, point to a role for VLN2 and VLN3 in coordinated cell elongation. Indeed, the organ twisting in *vlm2 vln3* results from subtle changes in cell size in opposite locations of the organs, which we show for root epidermal cells. It is not clear how villin-mediated actin filament bundling regulates coordinated cell expansion. We show that it does so by altering the organization of the actin cytoskeleton. The altered actin cytoskeleton organization in the double mutant might have effects on the direction of transport routes and/or the proper allocation of Golgi vesicles in the vicinity of the plasma membrane. In conclusion, our results show that villin is involved in the generation of thick actin filament bundles and suggest that these bundles are, directly or indirectly, important for coordinated cell expansion.

## MATERIALS AND METHODS

### Growth Conditions, Plant Strains, Allele Characterization, and Creation of Double Mutants

*Arabidopsis* (*Arabidopsis thaliana*) seeds were sterilized for 1 min with 70% ethanol, followed by a 3- to 5-min treatment with 15% to 20% household bleach (4% hypochlorite) and 0.05% Triton X-100. After sterilization, the seeds were stratified at 4°C for 2 to 4 d and germinated on one-half-strength Murashige and Skoog plates containing 0.7% agarose. After 1 week, seedlings were transplanted to potting compost. For live cell visualization of root epidermal cells, hypocotyl epidermal cells, and leaf pavement cells, seeds were germinated on one-half-strength Murashige and Skoog plates containing 1.5% agarose, which were placed at an oblique angle (approximately 15°–30° off vertical). For root hair imaging, seeds were sown on tilted coverslips containing a thin 0.7% agarose layer of Hoagland medium covered with biofoil (Vivascience). Root hairs grew along the coverslip and were imaged 3 to 4 d after planting. Colocalization of GFP:VLN3 and mCherry:FABD2 was performed by *Agrobacterium tumefaciens* injection in tobacco (*Nicotiana benthamiana*) leaves as described by Bouwmeester et al. (2011). All plants were grown at 25°C (16 h of light, 8 h of darkness).

The T-DNA insertion lines (both in the Col-0 background) for VLN2 (SAIL\_813\_H02) and VLN3 (SALK\_117097) were obtained from the Nottingham Arabidopsis Stock Centre (Scholl et al., 2000). Four- to 6-week-old leaves were used to isolate genomic DNA, which was used to confirm the T-DNA insertions (Supplemental Fig. S4) by PCR using the T-DNA left border-specific primer LB3 (for SAIL\_813\_H02) or LBA1 (for SALK\_117097) and VLN-specific primers (Supplemental Fig. S5; Supplemental Table S1) flanking the insertions. Homozygous mutants were identified in F3 progeny.

To analyze the expression of VLN2 and VLN3, RNA was extracted from leaves of the homozygous T-DNA insertion mutants using a Qiagen RNeasy Mini Kit. Total RNA was reverse transcribed into cDNA with SuperScript II Reverse Transcriptase (Invitrogen) and eluted in 20  $\mu$ L of diethyl pyrocarbonate-treated water. A volume of 1  $\mu$ L of the total cDNA was used in reverse transcription-PCR using primer combinations designed for coding regions before and after the T-DNA inserts (Supplemental Fig. S5; Supplemental Table S1).

### Complementation Analyses

Primers that included Gateway sequences (Invitrogen) were used to amplify genomic VLN3 including the promoter region (2,299 bp upstream

of the ATG) and the terminator region (1,228 bp including the stop codon), as annotated by The Arabidopsis Information Resource ([www.arabidopsis.org](http://www.arabidopsis.org)), which was recombined into pDONR207 (Invitrogen) followed by recombination into pMDC99 (Curtis and Grossniklaus, 2003). Genomic VLN3 including the promoter but lacking the headpiece-encoding region and the terminator region (which lacks the last 606 bp of the coding region of VLN3 including introns) was recombined into pDONR207, followed by a recombination into pMDC32 (Curtis and Grossniklaus, 2003), from which we deleted the 2 $\times$  35S promoter. The same adapted version of pMDC32 was used for the recombination of VLN2 including the promoter (3,902 bp upstream of the ATG) but lacking the stop codon and the terminator region.

To express GFP:VLN3 and GFP:VLN3 $\Delta$ H in the *vlm2 vln3* double mutant, genomic VLN3 lacking the promoter and terminator regions, as well as genomic VLN3 lacking the promoter, headpiece-encoding, and terminator regions, was amplified by PCR and recombined into pDONR207 followed by a recombination into pMDC43 (Curtis and Grossniklaus, 2003), from which the 2 $\times$  35S promoter was replaced by the endogenous VLN3 promoter. The same adapted version of pMDC43 was used for recombination (using pDONR221 [Invitrogen] as the entry clone) of coding sequences of VLN3 and VLN3 $\Delta$ H, which were amplified from cDNA. All constructs were transformed into the *vlm2 vln3* double mutant by *A. tumefaciens*-mediated transformation using the floral dip method (Clough and Bent, 1998). Primer sequences are shown in Supplemental Table S2.

### Phenotype Analysis and Confocal Microscopy

To visualize the actin cytoskeleton in the single mutants, we crossed the *vlm2* and *vln3* single mutants with wild-type Col-0 plants expressing *P35S::GFP::FABD* (Ketelaar et al., 2004). In the F2 generation, homozygous lines were identified by genotyping and selected for *GFP::FABD2* expression. A double mutant line with *GFP::FABD2* expression was obtained by *A. tumefaciens*-mediated transformation of *P35S::GFP::FABD2* into the *vlm2 vln3* double mutant using the floral dip method (Clough and Bent, 1998).

For live cell imaging of GFP:FABD2 and GFP:VLN3 localization, 3- to 5-d-old plants were used. Root hairs were imaged with a I-LAS Spinning Disk Confocal System (Roper Scientific) on a Nikon Eclipse Ti microscope using a 60 $\times$  (numerical aperture [N.A.] 1.4) oil-immersion objective. Root epidermal cells, hypocotyl epidermal cells, leaf pavement cells, and GFP:VLN3 and mCherry:FABD2 colocalization were imaged with an Axiovert 200M microscope (Zeiss) connected to a Zeiss LSM510 META confocal scanning system equipped with a 63 $\times$  (N.A. 1.4) oil-immersion objective. Cell dimensions of leaf and fruit stalk epidermal cells were imaged with a Nikon Eclipse 80i microscope, using a 10 $\times$  (N.A. 0.3) objective, and traced in ImageJ. Circularity reflects the ratio of cell area to cell perimeter and is defined as  $4\pi$  area/perimeter<sup>2</sup> (Brembu et al., 2004; Vidali et al., 2007).

The thickness of actin filament bundles was quantified by creating profiles of GFP fluorescence intensities of *P35S::GFP::FABD*-expressing hypocotyl cells, in the middle of Z projections of the cortical cytoplasm, perpendicular to the longitudinal cell axis (excluding the bright cell edges). To correct for differences in GFP:FABD2 intensity, we selected an area in which no actin filaments were visible and subtracted the mean fluorescence intensity of this region from the fluorescence intensities of the intensity profile. This resulted in a new plot profile, which was used to distribute the peaks in three classes: low (0–40 arbitrary units), medium (40–80 arbitrary units), and high (80–120 arbitrary units) gray levels (eight-bit files were used). Only peaks that were at least 10 units higher in fluorescence intensity than the intensities of the left and right bases of the peaks were included.

To determine skewness and occupancy of the actin cytoskeleton in hypocotyl epidermal cells and maximum intensity Z projections, we manually segmented cells such that cell borders were excluded. The resulting images were processed by using rolling-ball background subtraction (ball radius of 20 pixels) and Gaussian blurring (radius of 1 px). Further image analysis was performed as described by Higaki et al. (2010). For hypocotyl cells, sample sizes were 100 cells from seven different plants for Col-0 and 50 cells from 35 different plants for *vlm2 vln3*; for growing root epidermal cells, sample sizes were 50 cells from seven different plants for Col-0 and 35 cells from 20 different plants for *vlm2 vln3*. Two-tailed, unpaired *t* tests were used for the calculation of significance.

Sequence data from this article can be found in the GenBank/EMBL data libraries or The Arabidopsis Information Resource under accession numbers At2g41740 or NP\_565958.1 (Arabidopsis VLN2) and At3g57410 or NP\_567048.1 (Arabidopsis VLN3).

## Supplemental Data

The following materials are available in the online version of this article.

**Supplemental Figure S1.** Etiolated hypocotyls of the *vlm2 vlm3* double mutant curl (A and B), and root gravitropism is not affected in the *vlm2 vlm3* double mutant (C and D).

**Supplemental Figure S2.** Phenotype analysis of mutant complementation with different constructs.

**Supplemental Figure S3.** The mutations in VLN2 and VLN3 do not affect root hair growth.

**Supplemental Figure S4.** Molecular characterization of villin T-DNA insertion alleles.

**Supplemental Figure S5.** Locations of primers used for the molecular characterization of villin T-DNA insertion alleles.

**Supplemental Table S1.** Sequences of primers used for the molecular characterization of villin T-DNA insertion alleles.

**Supplemental Table S2.** Sequences of primers used for the complementation experiments and bacterial protein expression.

**Supplemental Movie S1.** Time-lapse recording of Col-0 and *vlm2 vlm3* double mutant plants.

**Supplemental Movie S2.** Time-lapse recording of GFP:VLN3 in root epidermal cells.

**Supplemental Movie S3.** Time-lapse recording of GFP:VLN3 in root hairs.

## ACKNOWLEDGMENTS

We thank Chris Staiger (Department of Biological Sciences, Purdue University) for the kind gift of the anti-lily villin antibody (Tominaga et al., 2000) and for sharing unpublished results and Dr. Takumi Higaki (Department of Integrated Biosciences, University of Tokyo) for help with determining the skewness parameter. Sjoerd Derksen (Wageningen University) is gratefully acknowledged for the images shown in Figure 2D, Klaas Bouwmeester (Laboratory of Phytopathology, Wageningen University) for help with the leaf infiltration experiments, and Ying Zhang (Laboratory of Cell Biology, Wageningen University) for assistance with root hair-growing experiments.

Received December 14, 2011; accepted December 21, 2011; published December 30, 2011.

## LITERATURE CITED

- Bartles JR** (2000) Parallel actin bundles and their multiple actin-bundling proteins. *Curr Opin Cell Biol* **12**: 72–78
- Bouwmeester K, de Sain M, Weide R, Gouget A, Klamer S, Canut H, Govers F** (2011) The lectin receptor kinase LecRK-I.9 is a novel Phytophthora resistance component and a potential host target for a RXLR effector. *PLoS Pathog* **7**: e1001327
- Brembu T, Winge P, Seem M, Bones AM** (2004) NAPP and PIRP encode subunits of a putative wave regulatory protein complex involved in plant cell morphogenesis. *Plant Cell* **16**: 2335–2349
- Bretscher A, Weber K** (1980) Villin is a major protein of the microvillus cytoskeleton which binds both G and F actin in a calcium-dependent manner. *Cell* **20**: 839–847
- Bryan J, Kurth MC** (1984) Actin-gelsolin interactions: evidence for two actin-binding sites. *J Biol Chem* **259**: 7480–7487
- Cheung AY, Wu HM** (2004) Overexpression of an *Arabidopsis* formin stimulates supernumerary actin cable formation from pollen tube cell membrane. *Plant Cell* **16**: 257–269
- Claessens MM, Semmrich C, Ramos L, Bausch AR** (2008) Helical twist controls the thickness of F-actin bundles. *Proc Natl Acad Sci USA* **105**: 8819–8822
- Clough SJ, Bent AF** (1998) Floral dip: a simplified method for Agrobacterium-mediated transformation of *Arabidopsis thaliana*. *Plant J* **16**: 735–743
- Collings DA, Wastneys GO, Miyazaki M, Williamson RE** (1994) Elongation factor 1 alpha is a component of the subcortical actin bundles of Characean algae. *Cell Biol Int* **18**: 1019–1024
- Curtis MD, Grossniklaus U** (2003) A Gateway cloning vector set for high-throughput functional analysis of genes in planta. *Plant Physiol* **133**: 462–469
- Favery B, Chelysheva LA, Lebris M, Jammes F, Marmagne A, De Almeida-Engler J, Lecomte P, Vaury C, Arkowitz RA, Abad P** (2004) *Arabidopsis* formin AtFH6 is a plasma membrane-associated protein upregulated in giant cells induced by parasitic nematodes. *Plant Cell* **16**: 2529–2540
- Geitmann A, Emons AM** (2000) The cytoskeleton in plant and fungal cell tip growth. *J Microsc* **198**: 218–245
- George SP, Wang Y, Mathew S, Srinivasan K, Khurana S** (2007) Dimerization and actin-bundling properties of villin and its role in the assembly of epithelial cell brush borders. *J Biol Chem* **282**: 26528–26541
- Glenney JR Jr, Geisler N, Kaulfus P, Weber K** (1981a) Demonstration of at least two different actin-binding sites in villin, a calcium-regulated modulator of F-actin organization. *J Biol Chem* **256**: 8156–8161
- Glenney JR Jr, Kaulfus P, Weber K** (1981b) F actin assembly modulated by villin: Ca<sup>++</sup>-dependent nucleation and capping of the barbed end. *Cell* **24**: 471–480
- Glenney JR Jr, Weber K** (1981) Calcium control of microfilaments: uncoupling of the F-actin-severing and -bundling activity of villin by limited proteolysis in vitro. *Proc Natl Acad Sci USA* **78**: 2810–2814
- Gungabissoon RA, Khan S, Hussey PJ, Maciver SK** (2001) Interaction of elongation factor 1alpha from *Zea mays* (ZmEF-1alpha) with F-actin and interplay with the maize actin severing protein, ZmADF3. *Cell Motil Cytoskeleton* **49**: 104–111
- Hampton CM, Liu J, Taylor DW, DeRosier DJ, Taylor KA** (2008) The 3D structure of villin as an unusual F-actin crosslinker. *Structure* **16**: 1882–1891
- Higaki T, Kutsuna N, Okubo E, Sano T, Hasezawa S** (2006) Actin microfilaments regulate vacuolar structures and dynamics: dual observation of actin microfilaments and vacuolar membrane in living tobacco BY-2 cells. *Plant Cell Physiol* **47**: 839–852
- Higaki T, Kutsuna N, Sano T, Kondo N, Hasezawa S** (2010) Quantification and cluster analysis of actin cytoskeletal structures in plant cells: role of actin bundling in stomatal movement during diurnal cycles in *Arabidopsis* guard cells. *Plant J* **61**: 156–165
- Holweg CL** (2007) Living markers for actin block myosin-dependent motility of plant organelles and auxin. *Cell Motil Cytoskeleton* **64**: 69–81
- Huang S, Robinson RC, Gao LY, Matsumoto T, Brunet A, Blanchoin L, Staiger CJ** (2005) *Arabidopsis* VILLIN1 generates actin filament cables that are resistant to depolymerization. *Plant Cell* **17**: 486–501
- Hussey PJ, Yuan M, Calder G, Khan S, Lloyd CW** (1998) Microinjection of pollen-specific actin-depolymerizing factor, ZmADF1, reorientates F-actin strands in *Tradescantia* stamen hair cells. *Plant J* **14**: 353–357
- Ketelaar T, Allwood EG, Anthony R, Voigt B, Menzel D, Hussey PJ** (2004) The actin-interacting protein AIP1 is essential for actin organization and plant development. *Curr Biol* **14**: 145–149
- Ketelaar T, de Ruijter NC, Emons AM** (2003) Unstable F-actin specifies the area and microtubule direction of cell expansion in *Arabidopsis* root hairs. *Plant Cell* **15**: 285–292
- Ketelaar T, Faivre-Moskalenko C, Esseling JJ, de Ruijter NC, Grierson CS, Dogterom M, Emons AM** (2002) Positioning of nuclei in *Arabidopsis* root hairs: an actin-regulated process of tip growth. *Plant Cell* **14**: 2941–2955
- Khurana P, Henty JL, Huang S, Staiger AM, Blanchoin L, Staiger CJ** (2010) *Arabidopsis* VILLIN1 and VILLIN3 have overlapping and distinct activities in actin bundle formation and turnover. *Plant Cell* **22**: 2727–2748
- Klahre U, Friederich E, Kost B, Louvard D, Chua NH** (2000) Villin-like actin-binding proteins are expressed ubiquitously in *Arabidopsis*. *Plant Physiol* **122**: 35–48
- Kovar DR, Gibbon BC, McCurdy DW, Staiger CJ** (2001) Fluorescently-labeled fimbrin decorates a dynamic actin filament network in live plant cells. *Planta* **213**: 390–395
- Kovar DR, Staiger CJ, Weaver EA, McCurdy DW** (2000) AtFim1 is an actin filament crosslinking protein from *Arabidopsis thaliana*. *Plant J* **24**: 625–636
- Le J, El-Assal Sel-D, Basu D, Saad ME, Szymanski DB** (2003) Requirements for *Arabidopsis* ATARP2 and ATARP3 during epidermal development. *Curr Biol* **13**: 1341–1347



- Li S, Blanchoin L, Yang Z, Lord EM (2003) The putative Arabidopsis arp2/3 complex controls leaf cell morphogenesis. *Plant Physiol* **132**: 2034–2044
- Mathur J, Mathur N, Kernebeck B, Hülskamp M (2003) Mutations in actin-related proteins 2 and 3 affect cell shape development in *Arabidopsis*. *Plant Cell* **15**: 1632–1645
- Mathur J, Spielhofer P, Kost B, Chua N (1999) The actin cytoskeleton is required to elaborate and maintain spatial patterning during trichome cell morphogenesis in *Arabidopsis thaliana*. *Development* **126**: 5559–5568
- Matova N, Mahajan-Miklos S, Mooseker MS, Cooley L (1999) Drosophila quail, a villin-related protein, bundles actin filaments in apoptotic nurse cells. *Development* **126**: 5645–5657
- Michelot A, Guerin C, Huang S, Ingouff M, Richard S, Rodiuc N, Staiger CJ, Blanchoin L (2005) The formin homology 1 domain modulates the actin nucleation and bundling activity of *Arabidopsis* FORMIN1. *Plant Cell* **17**: 2296–2313
- Miller DD, De Ruijter NCA, Bisseling T, Emons AMC (1997) From signal to form: aspects of the cytoskeleton-plasma membrane-cell wall continuum in root hair tips. *J Exp Bot* **48**: 1881–1896
- Miller DD, De Ruijter NCA, Bisseling T, Emons AMC (1999) The role of actin in root hair morphogenesis: studies with lipochito-oligosaccharide as a growth stimulator and cytochalasin as an actin-perturbing drug. *Plant J* **17**: 141–154
- Papuga J, Hoffmann C, Dieterle M, Moes D, Moreau F, Tholl S, Steinmetz A, Thomas C (2010) *Arabidopsis* LIM proteins: a family of actin bundlers with distinct expression patterns and modes of regulation. *Plant Cell* **22**: 3034–3052
- Scholl RL, May ST, Ware DH (2000) Seed and molecular resources for *Arabidopsis*. *Plant Physiol* **124**: 1477–1480
- Sheahan MB, Rose RJ, McCurdy DW (2007) Actin-filament-dependent remodeling of the vacuole in cultured mesophyll protoplasts. *Protoplasma* **230**: 141–152
- Shimmen T, Hamatani M, Saito S, Yokota E, Mimura T, Fusetani N, Karaki H (1995) Roles of actin filaments in cytoplasmic streaming and organization of transvacuolar strands in root hair cells of *Hydrocharis*. *Protoplasma* **185**: 188–193
- Staiger CJ, Hussey PJ (2004) Actin and actin-modulating proteins. In PJ Hussey, ed, *The Plant Cytoskeleton in Cell Differentiation and Development*. Blackwell Scientific Publications, Oxford, pp 32–80
- Staiger CJ, Yuan M, Valenta R, Shaw PJ, Warn RM, Lloyd CW (1994) Microinjected profilin affects cytoplasmic streaming in plant cells by rapidly depolymerizing actin microfilaments. *Curr Biol* **4**: 215–219
- Szymanski DB, Marks MD, Wick SM (1999) Organized F-actin is essential for normal trichome morphogenesis in *Arabidopsis*. *Plant Cell* **11**: 2331–2347
- Thomas C, Dieterle M, Gatti S, Hoffmann C, Moreau F, Papuga J, Steinmetz A (2008) Actin bundling via LIM domains. *Plant Signal Behav* **3**: 320–321
- Thomas C, Hoffmann C, Dieterle M, Van Troys M, Ampe C, Steinmetz A (2006) Tobacco WLIM1 is a novel F-actin binding protein involved in actin cytoskeleton remodeling. *Plant Cell* **18**: 2194–2206
- Thomas C, Moreau F, Dieterle M, Hoffmann C, Gatti S, Hofmann C, Van Troys M, Ampe C, Steinmetz A (2007) The LIM domains of WLIM1 define a new class of actin bundling modules. *J Biol Chem* **282**: 33599–33608
- Thomas C, Tholl S, Moes D, Dieterle M, Papuga J, Moreau F, Steinmetz A (2009) Actin bundling in plants. *Cell Motil Cytoskeleton* **66**: 940–957
- Tilney LG, Connelly PS, Vranich KA, Shaw MK, Guild GM (1998) Why are two different cross-linkers necessary for actin bundle formation in vivo and what does each cross-link contribute? *J Cell Biol* **143**: 121–133
- Tominaga M, Yokota E, Vidali L, Sonobe S, Hepler PK, Shimmen T (2000) The role of plant villin in the organization of the actin cytoskeleton, cytoplasmic streaming and the architecture of the transvacuolar strand in root hair cells of *Hydrocharis*. *Planta* **210**: 836–843
- Valster AH, Pierson ES, Valenta R, Hepler PK, Emons A (1997) Probing the plant actin cytoskeleton during cytokinesis and interphase by profilin microinjection. *Plant Cell* **9**: 1815–1824
- van der Honing HS, de Ruijter NC, Emons AM, Ketelaar T (2010) Actin and myosin regulate cytoplasm stiffness in plant cells: a study using optical tweezers. *New Phytol* **185**: 90–102
- Van Gestel K, Köhler RH, Verbelen JP (2002) Plant mitochondria move on F-actin, but their positioning in the cortical cytoplasm depends on both F-actin and microtubules. *J Exp Bot* **53**: 659–667
- Vidali L, Augustine RC, Kleinman KP, Bezanilla M (2007) Profilin is essential for tip growth in the moss *Physcomitrella patens*. *Plant Cell* **19**: 3705–3722
- Vidali L, Hepler PK (2001) Actin and pollen tube growth. *Protoplasma* **215**: 64–76
- Vidali L, Yokota E, Cheung AY, Shimmen T, Hepler PK (1998) The 135 kDa actin-bundling protein from *Lilium longiflorum* pollen is the plant homologue of villin. *Protoplasma* **209**: 283–291
- Wang HJ, Wan AR, Jauh GY (2008) An actin-binding protein, LILIM1, mediates calcium and hydrogen regulation of actin dynamics in pollen tubes. *Plant Physiol* **147**: 1619–1636
- Way M, Gooch J, Pope B, Weeds AG (1989) Expression of human plasma gelsolin in *Escherichia coli* and dissection of actin binding sites by segmental deletion mutagenesis. *J Cell Biol* **109**: 593–605
- Wu Y, Yan J, Zhang R, Qu X, Ren S, Chen N, Huang S (2010) *Arabidopsis* FIMBRIN5, an actin bundling factor, is required for pollen germination and pollen tube growth. *Plant Cell* **22**: 3745–3763
- Ye J, Zheng Y, Yan A, Chen N, Wang Z, Huang S, Yang Z (2009) *Arabidopsis formin3* directs the formation of actin cables and polarized growth in pollen tubes. *Plant Cell* **21**: 3868–3884
- Yokota E, Tominaga M, Mabuchi I, Tsuji Y, Staiger CJ, Oiwa K, Shimmen T (2005) Plant villin, lily P-135-ABP, possesses G-actin binding activity and accelerates the polymerization and depolymerization of actin in a Ca<sup>2+</sup>-sensitive manner. *Plant Cell Physiol* **46**: 1690–1703
- Yokota E, Vidali L, Tominaga M, Tahara H, Orii H, Morizane Y, Hepler PK, Shimmen T (2003) Plant 115-kDa actin-filament bundling protein, P-115-ABP, is a homologue of plant villin and is widely distributed in cells. *Plant Cell Physiol* **44**: 1088–1099
- Zhang H, Qu X, Bao C, Khurana P, Wang Q, Xie Y, Zheng Y, Chen N, Blanchoin L, Staiger CJ, et al (2010) *Arabidopsis* VILLIN5, an actin filament bundling and severing protein, is necessary for normal pollen tube growth. *Plant Cell* **22**: 2749–2767
- Zhang Y, Xiao Y, Du F, Cao L, Dong H, Ren H (2011) *Arabidopsis* VILLIN4 is involved in root hair growth through regulating actin organization in a Ca<sup>2+</sup>-dependent manner. *New Phytol* **190**: 667–682